

## Photoionization Study of the Sulfur Monoxide Radical Produced by Pyrolysis of Ethylene Sulfoxide

Eisuke NISHITANI, Kenichi FUKUDA, and Ikuzo TANAKA\*

Department of Chemistry, Tokyo Institute of Technology Ohokayama, Meguro-ku, Tokyo 152

(Received June 10, 1985)

Sulfur monoxide (SO) radical has been produced in the gas phase by pyrolysis of ethylene sulfoxide ( $\text{C}_2\text{H}_4=\text{SO}$ ) at  $510^\circ\text{C}$ . The vacuum ultraviolet photoionization efficiency curve between 915 and  $1220\text{ \AA}$  has been obtained for the first time. Several thermodynamic data about  $\text{C}_2\text{H}_4=\text{SO}$  have also been obtained from direct photoionization. The values of the bond energies of  $\text{D}_0(\text{C}_2\text{H}_4=\text{SO})$  and  $\text{D}_0(\text{C}_2\text{H}_4=\text{SO}^+)$  are  $4640 \pm 30$  and  $5160 \pm 30\text{ cm}^{-1}$  respectively. Ionization potentials (IP) of the  $\text{SO}(\text{X}^3\Sigma^-)$  radical and  $\text{C}_2\text{H}_4=\text{SO}$ , and the appearance potential (AP) of  $\text{SO}^+$  fragment ion from  $\text{C}_2\text{H}_4=\text{SO}$  are  $10.28 \pm 0.01$ ,  $9.49 \pm 0.02$ , and  $10.13 \pm 0.01\text{ eV}$ . In the system of  $\text{C}_2\text{H}_4=\text{SO}$ , the AP is lower than the IP and this phenomenon has only been found in this system.

The sulfur monoxide (SO) radical has been studied as an important intermediate in reactions involving oxygen atoms and molecules containing sulfur. It has also been found in interstellar space by radio telescopes.<sup>1)</sup> In addition, the SO radical is a very interesting radical from the point of electronic structure because of the isoelectronic species of diatomic sulfur ( $\text{S}_2$ ) and molecular oxygen ( $\text{O}_2$ ). In contrast to the large amount of spectroscopic data obtained for  $\text{O}_2$ , SO, and  $\text{S}_2$  in several low-lying electronic states,<sup>2)</sup> our current knowledge concerning the SO radical in the vacuum ultraviolet region is very limited. Though autoionization in radicals has been rarely observed in this region so far, it is expected that the autoionization peaks might appear in the SO radical because of the similarity to  $\text{O}_2$ .

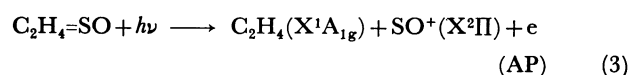
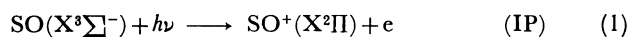
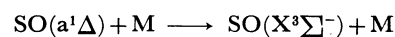
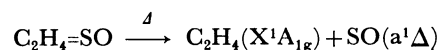
Since the far ultraviolet absorption spectrum of  $\text{O}_2$  was observed by Price and Collins in 1935,<sup>3)</sup> absorption spectra, the photoionization efficiency curves and photoelectron spectra of  $\text{O}_2$  have been intensively studied. A high resolution (FWHM  $0.07\text{ \AA}$ ) photoionization study of  $\text{O}_2$  has been carried out by Dehmer and Chupka.<sup>4)</sup> For the  $\text{S}_2$  radical, the relative photoionization efficiency curve has been observed by Berkowitz *et al.*<sup>5)</sup> in the gas phase by thermal vaporization of  $\text{HgS}$ . They found that an autoionization structure emerged, but the peak shapes were not clear enough to allow spectroscopic studies.

Compared to the study of these species, at the present stage, very few works have been carried out on the SO radical in the vacuum ultraviolet region. Donovan *et al.*<sup>6)</sup> have obtained the absorption spectrum of the SO radical and studied the Rydberg series (The  $\text{D}^3\Pi$  and  $\text{E}^3\Pi$  states) converging to the  $\text{X}^2\Pi$  state of  $\text{SO}^+$ . The photoelectron spectrum of the SO radical produced by discharge of  $\text{CS}_2$  and  $\text{O}_2$  was also observed by Jonathan *et al.* in 1974.<sup>7)</sup>

The present work reports the first mass spectrometric analysis of the relative photoionization efficiency curve of the SO radical produced by pyrolysis of ethylene sulfoxide ( $\text{C}_2\text{H}_4=\text{SO}$ ). The synthesis of  $\text{C}_2\text{H}_4=\text{SO}$ <sup>8)</sup> and production of the SO radical by its pyrolysis has been reported.<sup>9)</sup> Also the  $\text{a}^1\Delta$  state of

the SO radical produced by pyrolysis of  $\text{C}_2\text{H}_4=\text{SO}$  was analyzed from the microwave spectrum by Saito in 1970.<sup>10)</sup>

The pyrolysis and photoionization in the present system are described below:



From the threshold energies for above processes, the bond energies of  $\text{D}_0(\text{C}_2\text{H}_4=\text{SO})$  and  $\text{D}_0(\text{C}_2\text{H}_4=\text{SO}^+)$  were determined. The IP of the SO radical in process (1) obtained from mass spectrometric photoionization is in excellent agreement with the results of photoelectron studies<sup>7)</sup> and photofragmentation studies of sulfur dioxide.<sup>11)</sup> The IP of  $\text{C}_2\text{H}_4=\text{SO}$  in process (2) and the AP of  $\text{SO}^+$  from  $\text{C}_2\text{H}_4=\text{SO}$  in process (3) were obtained. Thus, these threshold energies indicate that the AP of  $\text{SO}^+$  from  $\text{C}_2\text{H}_4=\text{SO}$  should be lower than the IP of the SO radical. This unique phenomenon was first observed in the system of  $\text{C}_2\text{H}_4=\text{SO}$ .

On the other hand, in process (1) the relative photoionization efficiency curve of the SO radical was obtained by scanning the excitation wavelength. Rather strong autoionization peaks were observed on this curve. But these peaks could not be assigned due to the lack of strong vibrational progressions such as are found for  $\text{O}_2^+$ .

### Experimental

The experimental arrangement is shown in Fig. 1. The apparatus consisted of a hydrogen discharge light source operated at  $0.4\text{ A}$  dc with about  $700\text{ V}$  across the tube, a  $50\text{ cm}$  Seya-Namioka type vacuum monochromator with a resolution of  $2.3\text{ \AA}$  (FWHM) which dispersed and refocused the monochromatic light into the ionization chamber, a set of

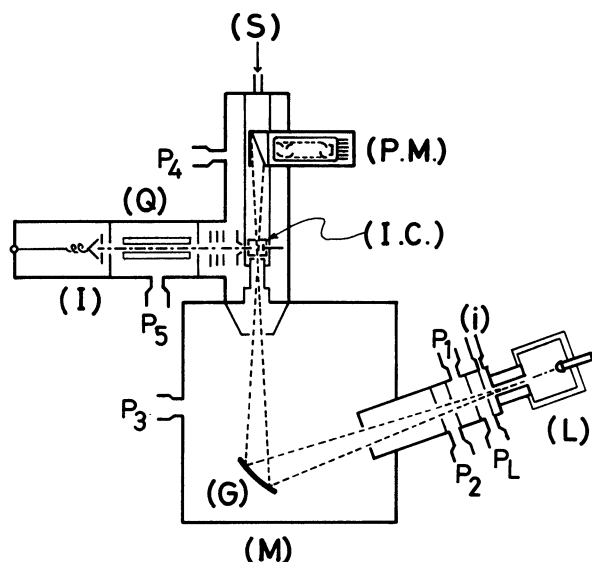


Fig. 1. Schematic diagram of the experimental apparatus. L; light source, i; gas inlet, G; grating, M; monochromator, I.C.; ionization chamber, Q; quadrupole mass filter, P.M.; photon monitor, I; ion multiplier, S; sample gas inlet, P<sub>L</sub>, P<sub>1</sub>—P<sub>5</sub>; differential pumping system.

ion extraction and focusing lenses, and a quadrupole mass spectrometer (NEVA NAG-520) for ion detection.

Ion counts were measured by an electronmultiplier (Murata EMS-6081B), and photon counts were measured by the scintillation counter of a photomultiplier (HTV R-268) coated with sodium salicylate. After each signal had been amplified and identified by a fast pre-amplifier (ORTEC 9301) and an amplifier-discriminator (ORTEC 9302), it was integrated by the counter (ORTEC 9315). The accumulation of signals and control of the experimental apparatus were regulated by a microcomputer (NEC PC-9801). The relative photoionization efficiency was derived by the normalization method, dividing the ion counts by the photon counts.

In order to obtain radicals by pyrolysis, a tape-heater wrapped around a 10mm diameter quartz tube was used at about 20cm upstream from the ionization chamber. The temperature was varied in the region between room temperature and 580°C. The total pressure was measured by a capacitance manometer (MKS-Baratron). The sample pressure was typically about 0.6 mTorr in the ionization chamber.

In order to investigate the temperature dependence of pyrolysis of C<sub>2</sub>H<sub>4</sub>=SO, ion counts for several species were measured in the range, room temperature to 580°C. The sample was irradiated by light at 1160.3 Å, whose energy is higher than either of the IPs of the parent molecule or ethylene produced by pyrolysis, but it was lower than the AP of the fragment ethylene ion from the parent molecules. The SO<sup>+</sup> radical ion could not be used for monitoring the pyrolysis because its IP is higher than the AP of the SO<sup>+</sup> fragment ion from the parent molecules. The temperature dependence of ion counts produced by irradiation at 1160.3 Å is shown in Fig. 2. At 300°C, the ion counts of C<sub>2</sub>H<sub>4</sub>=SO<sup>+</sup> were reduced to one-half of those at room temperature. With a further rise in the temperature, they were rarely observed. On the other hand, ion counts of ethylene increased up to 500°C,

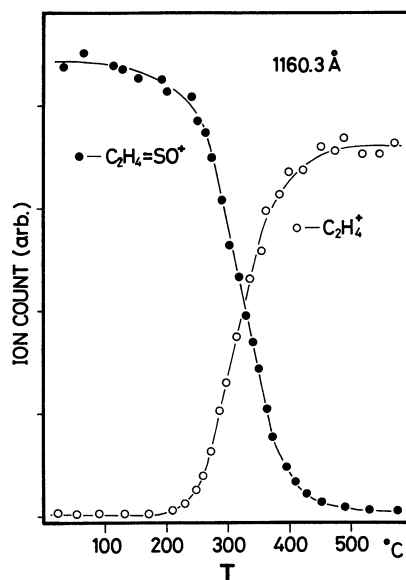


Fig. 2. Temperature variation of the ion counts of C<sub>2</sub>H<sub>4</sub>=SO and C<sub>2</sub>H<sub>4</sub>. ● denotes the ion counts of C<sub>2</sub>H<sub>4</sub>=SO, ○ denotes the ion counts of C<sub>2</sub>H<sub>4</sub> produced by pyrolysis from C<sub>2</sub>H<sub>4</sub>=SO.

and above 500°C they remained stationary. Thus, the temperature of the pyrolysis was maintained at 510°C throughout this experiment.

## Results and Discussion

The relative photoionization efficiency curve of SO<sup>+</sup> from the SO radical for the wavelength region 915—1220 Å, is shown in Fig. 3, where the hydrogen discharge lamp was used as a source at a wavelength resolution (FWHM) of 2.3 Å. In the present experiment, the accuracy of the wavelength was determined to be within about 0.5 Å from H Lyman-α and H Lyman-β in the light source. For excited O<sub>2</sub>(a<sup>1</sup>Δ<sub>g</sub>), Jonathan *et al.*<sup>13</sup> examined the photoelectron spectrum of the (2Δ<sub>g</sub>←1Δ<sub>g</sub> and 2Φ<sub>u</sub>←1Δ<sub>g</sub>) ionization transition using phase-sensitive detection. These transitions from the a<sup>1</sup>Δ state could not be being observed in the present photoionization efficiency curve, the reason that the excited SO(a<sup>1</sup>Δ) may have almost completely been deactivated. The photoionization efficiency rises sharply at 1206.3±0.5 Å (=10.28±0.01 eV), and above this threshold there is a gradual increase in ionization cross section. Somewhat strong peaks, assigned to autoionization structures, have been detected between 1010 and 920 Å from which the autoionization structures have been determined. But along the SO<sup>+</sup> photoionization curve there are no very strong vibrational progressions like O<sub>2</sub><sup>+</sup> between 1005 Å (the threshold of IP) and 850 Å.<sup>4</sup> Therefore, spectroscopic studies could not be done as successfully of the autoionization peaks in SO<sup>+</sup> as those of the broad ones S<sub>2</sub><sup>+</sup>.<sup>5</sup>

Furthermore, to obtain various thermodynamic data

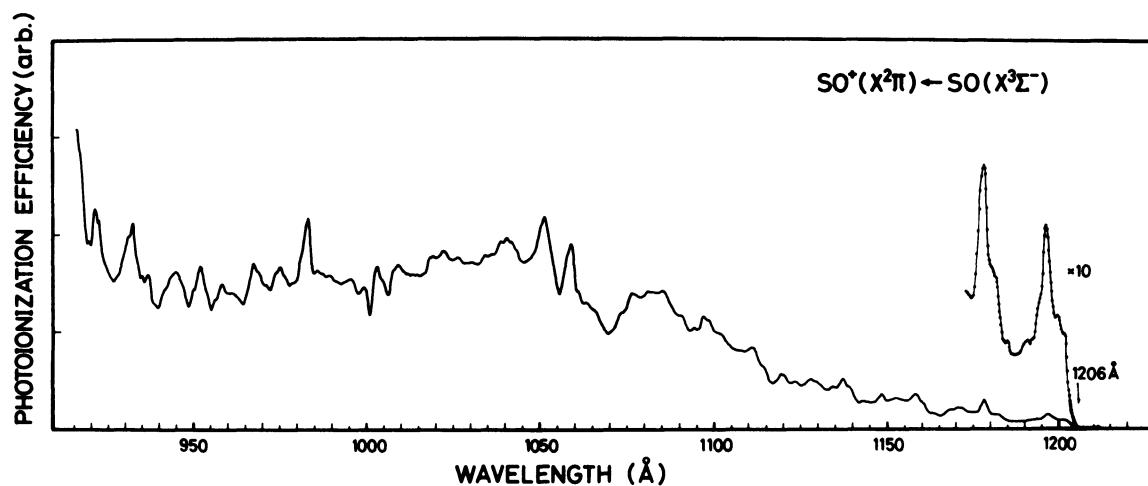


Fig. 3. Photoionization efficiency curve for  $\text{SO}^+$  from the SO radical taken between 1220 and 915 Å at a wavelength resolution (FWHM) of 2.3 Å at 510°C.

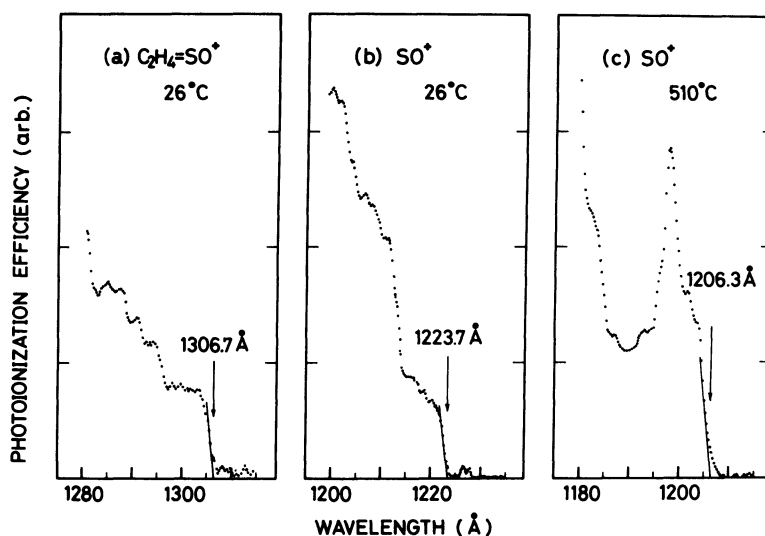


Fig. 4. The relative photoionization cross sections in the neighborhood of the threshold energies.

(a) The ion counts of  $\text{C}_2\text{H}_4=\text{SO}^+$  at the room temperature, (b) The ion counts of  $\text{SO}^+$  fragment ion from  $\text{C}_2\text{H}_4=\text{SO}$  at room temperature, (c) The ion counts of the SO radical at 510°C.

TABLE 1. SUMMARY OF PHOTOIONIZATION DATA FOR THE SYSTEM OF ETHYLENE SULFOXIDE

Ion	Threshold	Process	Temperature
	eV <sup>a)</sup>		°C
$\text{SO}^+$	$10.28 \pm 0.01$	$\text{SO}(\text{X}^3\Sigma^-) + h\nu \rightarrow \text{SO}^+(\text{X}^2\Pi) + e$	510
$\text{SO}^+$	$10.13 \pm 0.01$	$\text{C}_2\text{H}_4=\text{SO} + h\nu \rightarrow \text{C}_2\text{H}_4(\text{X}^1\text{A}_{1g}) + \text{SO}^+(\text{X}^2\Pi) + e$	26
$\text{C}_2\text{H}_4=\text{SO}^+$	$9.49 \pm 0.02$	$\text{C}_2\text{H}_4=\text{SO} + h\nu \rightarrow \text{C}_2\text{H}_4=\text{SO}^+ + e$	26

a) Estimated uncertainties.

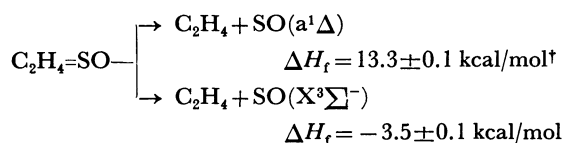
relating to  $\text{C}_2\text{H}_4=\text{SO}$ , the threshold energies were measured. Figure 4 shows the relative photoionization cross section of (a)  $\text{C}_2\text{H}_4=\text{SO}$  at room temperature, (b)  $\text{SO}^+$  fragment ion from  $\text{C}_2\text{H}_4=\text{SO}$  at room temperature, (c)  $\text{SO}^+$  ionized directly from the SO radical at 510°C.  $\text{C}_2\text{H}_4^+$  fragment ions at room temperature were not observed. These threshold energies are summarized in

Table 1.

The IP of SO in the present work is in excellent agreement with the value of  $10.29 \pm 0.02$  eV obtained from photoelectron spectra by Jonathan *et al.*<sup>7)</sup> and that of 10.21 eV obtained from the photofragmentation method by Dibeler and Liston.<sup>11)</sup> Though, it was assumed that  $\text{SO}^+$  ions might appear from  $\text{SO}(\text{a}^1\Delta)$

produced by pyrolysis of  $C_2H_4=SO$  in the region longer than  $1206.3 \text{ \AA}$  ( $=10.28 \text{ eV}$ ) by means of an allowed  $SO^+(X^2\Pi) \leftarrow SO(a^1\Delta)$  ionization transition, in fact,  $SO^+$  ions were not observed in this region as can be seen in Fig. 4(c). This results from the fact that the excited  $SO(a^1\Delta)$  was almost completely deactivated to the ground state before it reached to the ionization chamber.

The AP of  $SO^+$  fragment ion from  $C_2H_4=SO$  and the IP of  $C_2H_4=SO$  were determined. It is worth noting that the IP of the  $SO$  radical is about  $0.15 \text{ eV}$  higher than the AP of  $SO^+$  from  $C_2H_4=SO$ . In the pyrolysis of  $C_2H_4=SO$  described in process (1),  $C_2H_4=SO$  must correlate to  $SO(a^1\Delta)$  from spin conservation, thus decomposition to  $C_2H_4+SO(a^1\Delta)$  is an endothermic reaction. The values of  $\Delta H_f$  in the following reactions are derived by using the transition energy of  $SO(a^1\Delta \leftarrow X^3\Sigma^-)$  from chemiluminescence studies of Barnes *et al.*<sup>12)</sup>



The transitions to  $SO^+(X^2\Pi)$  from both  $SO(a^1\Delta)$  and  $SO(X^3\Sigma^-)$  are allowed. It seems that the exothermicity of the reaction in pyrolysis contributes to the ionization of  $SO$  from parent molecule. Therefore, it stands to reason that the AP of  $SO^+$  from  $C_2H_4=SO$  is lower than the IP of the  $SO$  radical. From these results and the IP of  $C_2H_4=SO$ , the following bond energies of  $D_0(C_2H_4=SO)$  and  $D_0(C_2H_4=SO^+)$  were obtained;

$$D_0(C_2H_4=SO) = 4640 \pm 30 \text{ cm}^{-1}$$

$$D_0(C_2H_4=SO^+) = 5160 \pm 30 \text{ cm}^{-1}$$

Furthermore, from a consideration of the temperature dependence of  $C_2H_4=SO$ , the activation energy in the system of  $C_2H_4=SO$  has been estimated.

This reaction is regarded as a first-order irreversible unimolecular decomposition reaction of the plug type, and, so, the following equation in logarithmic form is obtained;

$$\ln(C_0/C) = (k/v)l, \quad (4)$$

where  $C_0$  and  $C$  are sample concentrations of the entrance and exit regions of the pyrolysis tube, respectively, and  $k$  is the rate constant,  $v$  is the flow rate, and  $l$  is the length of the pyrolysis tube. From the expressions for the rate constant,  $k$  expressed in terms of the frequency factor  $A$ , and the activation energy  $E$ , we obtain the following equation;

$$\ln(\ln(C_0/C)) = -E/RT + \ln A/v. \quad (5)$$

<sup>†</sup>  $1 \text{ cal}_{th} = 4.184 \text{ J}$ .

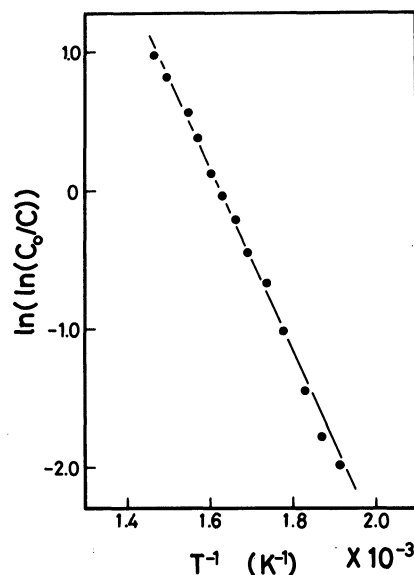


Fig. 5. Arrhenius plot of  $\ln(\ln(C_0/C))$  versus  $T^{-1}$  obtained from the ion counts of  $C_2H_4=SO^+$  in Fig. 2.

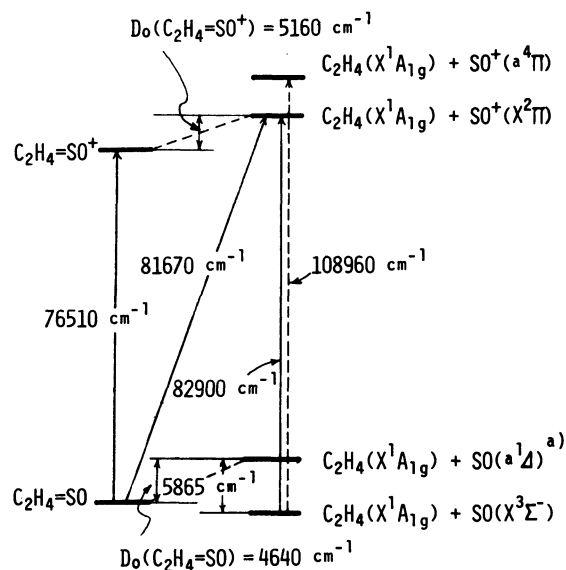


Fig. 6. The energy diagram of  $C_2H_4=SO$  and  $SO$ . a) The energy difference between  $a^1\Delta$  and  $X^3\Sigma^-$  from Ref. 12.

Then the plot of  $\ln(\ln(C_0/C))$  versus  $T^{-1}$  will yield the activation energy  $E$  from slope of the curve.

The plot of  $\ln(\ln(C_0/C))$  versus  $T^{-1}$  which was obtained from the ion counts of  $C_2H_4=SO^+$  in Fig. 2 is shown in Fig. 5. The activation energy was estimated to be  $13.6 \text{ kcal/mol}$  and was in excellent agreement with the value of  $D_0(C_2H_4=SO)$  obtained from the above discussion.

The energy diagram of  $C_2H_4=SO$  and  $SO$  is summarized in Fig. 6.

Although the electronic state of  $C_2H_4=SO$  has not yet been studied, it is presumed that the electron in the highest occupied molecular orbital is an antibonding electron because the bond energy of the neutral state is

less than that of the ionic state.

The authors would like to thank Dr. S. Saito of Institute for Molecular Science for preparing ethylene sulfoxide.

#### References

- 1) C. A. Gottlieb and J. A. Ball, *Astrophys. J.*, **184**, L59 (1973); **187**, L47 (1974).
  - 2) a) W. C. Swope, Y. P. Lee, and H. F. Schafer III, *J. Comput. Phys.*, **26**, 243 (1978); *J. Chem. Phys.*, **70**, 947 (1979); **71**, 3761 (1979); b) G. Theodorakopoulos, S. D. Peyerimhoff, and R. J. Bunker, *Chem. Phys. Lett.*, **81**, 413 (1981).
  - 3) W. C. Price and G. Collins, *Phys. Rev.*, **48**, 714 (1935).
  - 4) P. M. Dehmer and W. A. Chupka, *J. Chem. Phys.*, **62**, 4525 (1975).
  - 5) J. Berkowitz and C. Lifshitz, *J. Chem. Phys.*, **48**, 4346 (1968).
  - 6) a) R. J. Donovan, D. Husan, and P. T. Jackson, *Trans. Faraday Soc.*, **65**, 2930 (1969); b) R. J. Donovan and D. J. Little, *Spectrosc. Lett.*, **4**, 213 (1971).
  - 7) a) N. Jonathan, D. J. Smith, and K. J. Ross, *Chem. Phys. Lett.*, **9**, 217 (1971); b) J. M. Dyke, L. Golob, N. Jonathan, A. Morris, M. Okuda, and D. J. Smith, *J. Chem. Soc., Faraday Trans. 2*, **70**, 1818 (1974).
  - 8) K. Kondo and A. Negishi, *Tetrahedron*, **27**, 4821 (1971).
  - 9) S. Saito, *Bull. Chem. Soc. Jpn.*, **42**, 667 (1969).
  - 10) S. Saito, *J. Chem. Phys.*, **53**, 2544 (1970).
  - 11) V. H. Dibeler and S. K. Liston, *J. Chem. Phys.*, **49**, 482 (1968).
  - 12) I. Barnes, K. H. Becker, and E. H. Fink, *Chem. Phys. Lett.*, **67**, 310 (1979).
  - 13) N. Jonathan, A. Morris, M. Okuda, K. J. Ross, and D. J. Smith, *J. Chem. Soc., Faraday Trans. 2*, **70**, 1810 (1974).
-